Green Chemistry

This article can be cited before page numbers have been issued, to do this please use: Y. Duan, T. Song, X. Dong and Y. Yang, *Green Chem.*, 2018, DOI: 10.1039/C8GC00619A.

View Article Online
DOI: 10.1039/C8GC00619A

Journal Name

ARTICLE

Received 00th January 20xx,
Accepted 00th January 20xx

DOI: 10.1039/x0xx00000x

www.rsc.org/

Enhanced Catalytic Performance of Cobalt Nanoparticles Coated by a N,P-Codoped Carbon Shell Derived from Biomass for Transfer Hydrogenation of Functionalized Nitroarenes

Yanan Duan, Tao Song, Xiaosu Dong, and Yong Yang*

The development of abundantly available base metal catalysts for organic transformations remains an important goal of chemical research. Herein, we report the first facile fabrication of an active, inexpensive, and reusable cobalt nanoparticles (NPs) coated by a N,P-codoped carbon shell derived from naturally renewable biomass and earth-abundant, low-cost cobalt salt and PPh_3. The entire process is operationally simple and straightforward, cost-effective and environmentally benign and can be in mass production for practical application. The resultant catalysts allow for highly efficient and selective transfer hydrogenation of functionalized nitroarenes to the corresponding anilines using formic acid or ammonium formate as hydrogen donor. Uniformly incorporated N and P into the carbon lattices played synergistic effects with the encapsulated Co NPs to engineer the structure and composition of the catalyst, thereby substantially boosting the catalytic efficiency. The most active catalyst Co@NPC-800 exhibited outstanding activity and exclusive selectivity for reduction of functionalized nitroarenes to anilines, especially for those decorating with readily reducible functional groups. The catalyst demonstrated high stability and can be easily separated by using external magnet for successive reuses without significant loss in both activity and selectivity.

Introduction

Anilines and its derivatives are an important class of compounds used as building blocks in the manufacture of dyes, agrochemicals, pigments, pharmaceuticals, and polymers.[1] Owing to their immense utility, the development of novel methods for the synthesis of anilines continues to be an active area of research. Among all known developed methods, direct reduction of nitroarenes catalyzed by noble metal catalysts with molecular hydrogen represents the most straightforward and atom-economic process.[2] However, such process is usually conducted at high pressure and temperature, which significantly restricts its wider application due to the need for specialized equipment and potential safety issues regarding H_2 handling accompanying with high energy consumption. More worse, the process generally demonstrates poor chemoselectivity for hydrogenation of functionalized nitroarenes bearing with diverse and readily reducible functional groups,[3] where the resulting anilines constitute key intermediates for the synthesis of fine and bulk chemicals, especially in life science applications.

As a complement to catalytic hydrogenation with molecular hydrogen, catalytic transfer hydrogenation of nitroarenes with hydrogen-donor such as formic acid,[4a,b] sodium borohydride,[4c] ammonia borane,[4d] alcohol,[4e] and hydrazine[4f] has received considerable attention because of their operational simplicity, better control of chemoselectivity and good compatibility with functional groups under mild conditions. As a consequence, a number of well-defined homogeneous metal complexes and stable heterogeneous metal-based catalysts have been developed for catalytic transfer hydrogenation of nitroarenes over the last decade.[5] Obviously, from both economic and environmental perspectives, non-noble metal-based heterogeneous catalysts significantly stand out due to their integrated advantages such as earth-abundant, low-cost and low-toxicity, stability, recyclability and easy separation as well. In this regard, Beller and co-workers developed a novel heterogeneous catalyst in which cobalt nanoparticles (NPs) are embedded in a N-doped carbon matrix by direct carbonization of non-volatile molecularly defined Co-amine ligated complexes for a general reduction of all kinds of nitroarenes with outstanding catalytic performance in 2013.[6] After their seminal work, several beautiful N-doped carbon supported cobalt-based catalysts have been successively developed for highly active and selective hydrogenation of functionalized nitroarenes by several independent research groups.[7] These cobalt based N-doped carbon catalysts were generally synthesized via pyrolysis of either molecularly well-defined complexes together with inert supports (e.g., SiO_2, graphene, porous carbon, or carbon nanotubes) or pre-prepared metal organic framework precursors (MOFs). In some cases, the subsequent etching of SiO_2 templates with acid or base aqueous solution after pyrolysis is required to generate the desired molecularly single active sites.[4a,8] Nonetheless, intensive studies disclosed that N-doped carbon supports not only can effectively protect active cobalt NPs from harsh environments and strongly resist NPs aggregation to enhance the durability, but also exert a

---

CAS Key Laboratory of Bio-Based Materials
Qingdao Institute of Bioenergy and Bioprocess Technology
Chinese Academy of Sciences, Qingdao 266101, China
E-mail: yangyong@qibebt.ac.cn

†Electronic Supplementary Information (ESI) available: The details of catalyst preparation, characterization, and control experiment results. See DOI: 10.1039/x0xx00000x

View Article Online
DOI: 10.1039/C8GC00619A

synergistic effect with cobalt NPs to substantially boast catalytic activity and selectivity of these catalysts.

Despite such elegant achievements, the necessity of either the use of sophisticated and expensive organic ligands, or tedious and multi-step synthesis of sacrificial template materials accompanied with uneconomical and inapplicable in mass production, or emission of large amount of wastes in the preparation process constitutes a serious drawback. To solve these issues, attention is being emergingly turned to the naturally renewable and available biomass in combination with inexpensive and earth-abundant metal salts to prepare the N-based carbon supported catalysts,[9] which represents an important aspect of sustainable chemical research. Very recently, we developed a facile, green and eco-friendly synthetic method to fabricate N-doped hierarchical porous carbon using bamboo shoots as N and C sources, in which nearly 8 wt% of N-containing compounds (e.g., proteins and amino acids) in its composition can be ideally offered as N source as dopant. The resulting carbon served as an excellent support for immobilization of palladium nanoparticles to form a recyclable and efficient heterogeneous catalyst for chemoselective semihydrogenation and hydrosilylation of alkynes.[10]

Bearing these results in mind, we envision that complexation of cobalt salt with bamboo shoots can be used for generation of cobalt NPs dispersed on N-doped carbon. Meanwhile, to further modify and/or enrich the characteristics of carbon shell, a more electronegative P atom was introduced simultaneously using cheap and easily available PPh_3 as P source during complexation for in-situ growth of cobalt NPs encapsulated with N,P-dual doped carbon matrix upon pyrolysis. To our surprise, we found that the second P-dopant in the catalyst pronouncedly improve the reaction efficiency compared with the counterpart with sole N-dopant. Herein, for the first time, we report a novel nanostructured cobalt NPs coated by a N,P-codoped carbon shell (hereafter referred to as Co@NPC-x, where x denotes the pyrolysis temperature), which are synthesized via a cost-effective and environmentally benign method using naturally renewable and easily available biomass together with earth-abundant and cheap cobalt salts. The obtained catalyst exhibited outstanding activity and exclusive selectivity for catalytic transfer hydrogenation of functionalized nitroarenes using formic acid (FA) or ammonium formate as hydrogen donor. A broad variety of functionalized nitroarenes can be efficiently reduced to their corresponding anilines with excellent tolerance of functional groups. The catalyst also demonstrates high stability and can be easily separated using simple external magnet for at least 6 successive reuses without significant loss in both activity and selectivity.

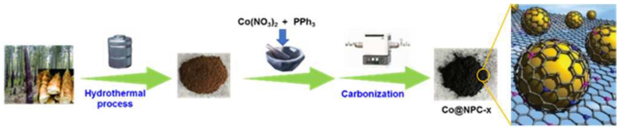

Figure 1. Schematic illustration of the preparation of Co NPs coated by N,P-codoped carbon shell.

Table 1. Catalytic performance with different catalysts[a]

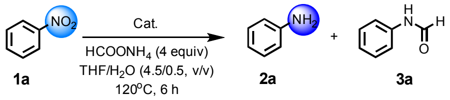

Entry	Catalyst	Time (h)	Conversion (%)[b]	Selectivity (%)[b]	
				2a	3a
1	Co@C-800	6(12)	8(49)	100(98)	0(2)
2	Co@NC-800	6(12)	41(95)	100(97)	0(3)
3	Co@NPC-700	12	75	95	5
4	Co@NPC-800	6(12)	97(100)	98(97)	2(3)
5	Co@NPC-900	12	100	89	11
6[c]	AC-800	12	0.5	100	0
7[c]	NC-800	12	6	100	0
8[c]	NPC-800	12	22	100	0
9	no	12	0	-	-
10	$Co(NO_3)_2$	12	0.2	100	0

[a]Reaction conditions: nitrobenzene (0.5 mmol), $HCOONH_4$ (2.0 mmol), catalyst (4.8 mol% of Co), THF/H_2O (5 mL, 4.5/0.5, v/v), 120°C. [b]determined by GC-FID using dodecane as an internal standard.[c]40 mg of the supports was used.

Results and discussion

The catalysts Co@NPC-x were prepared in a sequential hydrothermal and pyrolysis procedure (Figure 1, see details in the Supporting Information). Briefly, the fresh bamboo shoots were firstly cut into slices, dried and ground into powder followed by the hydrothermal process to get the brown solids. The resulting solids were homogeneously mixed with $Co(NO_3)_2$ and PPh_3 followed by pyrolysis under N_2 atmosphere at varying temperature. The Co content in catalysts was determined to be 2.14 ~ 4.04 wt% by the coupled plasma optical emission spectrometry (ICP-OES) (Table S7, Supporting Information). For reference, the catalyst Co@NC with sole N-dopant, Co@C without N and P dopant by direct pyrolysis of the mixture of activated carbon and cobalt salt, and the bare supports NPC and NC without metal loading were also prepared with similar procedure, respectively.

The obtained catalysts were investigated for catalytic transfer hydrogenation of functionalized nitroarenes in the presence of various hydrogen donors. Transfer hydrogenation of nitrobenzene was chosen as benchmark reaction, and upon intensively screening of a set of factors including solvent, temperature, amount of catalyst loading, type of hydrogen donors (e.g., FA, ammonium formate, $NaBH_4$, or hydrosilane ($PhMe_2SiH$)) and their amounts employed with respect to nitrobenzene (see Table S1-6 in Supporting Information), we found that the best catalytic performance was achieved with complete conversion and excellent selectivity to aniline (up to 97%) using THF/H_2O (5 mL, 4.5/0.5, v/v) as solvent, 4 equivalent of ammonium formate at 120°C in the presence of 40 mg of Co@NPC-800 within 12 h. Notably, both FA and ammonium formate, which are easily accessible from biomass processing with high hydrogen capacity and attractive features of

View Article Online
DOI: 10.1039/C8GC00619A

convenient storage and delivery, can serve as ideal hydrogen donors for the reduction, while ammonium formate distinctly exhibited superior efficiency to FA under identical conditions. Control experiment reveals that the reaction proceeded quite smoothly to achieve 96% conversion of nitrobenzene in the first 6 h, while it took another 6 h for complete conversion.

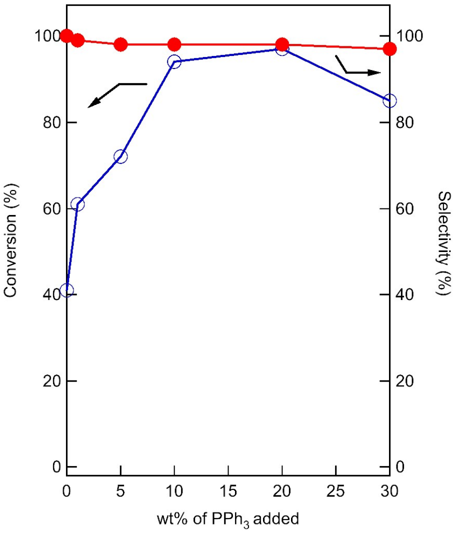

Figure 2. The catalytic performance as a function of the added amount of PPh_3 in the catalyst Co@NC-800.
Reaction conditions: nitrobenzene (0.5 mmol), $HCOONH_4$ (2.0 mmol), constant cobalt contents (4.8 mol% of Co) in the selected catalysts, THF/H_2O (5 mL, 4.5/0.5, v/v), 120°C, 6 h under nitrogen atmosphere.

Meanwhile, several other features are noticeably observed upon reaction conditions optimization (Table 1). Firstly, the pyrolysis temperature for the resulting catalysts Co@NPC had a considerable impact on the catalytic performance. The catalyst Co@NPC-700 gave inferior reaction efficiency than that of Co@NPC-800, while an appreciable lower selectivity to aniline was achieved in the presence of Co@NPC-900 (entries 3-5). The catalyst Co@NPC-800 showed maximum performance in terms of both activity and selectivity. Secondly, heteroatoms doping in the carbon framework of the catalysts remarkably boosted the reaction efficiency. The catalysts Co@C-800 and Co@NC-800 were respectively employed with identical molar percentage of cobalt (equals to Co@NPC-800) for the reduction (entries 1 & 2). Under otherwise identical conditions, only 8% conversion was achieved with the catalyst Co@C-800 after 6 h, while the catalyst Co@NC-800 gave 41% conversion and is 4 times higher than that of Co@C-800. More impressively, nearly complete conversion of nitrobenzene was observed for the catalyst Co@NPC-800. Apparently, the reaction efficiency follows the order of Co@NPC-800 > Co@NC-800 > Co@C-800. Such results clearly indicate that heteroatom N or N,P in the carbon framework exerted a vital role for the reduction. This is indeed the case and was further verified by the reaction by using an inert activated carbon (AC), NC-800, and NPC-800 as catalyst, respectively (entries 6-8). The reaction did not proceed in the presence of AC, while NC-800 and NPC-800 gave 6 and 22% conversion of nitrobenzene to aniline, respectively. A sharp increase in activity was distinctly observed for these carbon supports with heteroatoms modification while their efficiency was not comparable to the level of their analogues with Co NPs loading. In addition, such unique nanostructured cobalt NPs encapsulated in the heteroatom-doped carbon shells is the essential for this transfer hydrogenation reaction. The reaction completely shut down with either the absence of the catalyst or cobalt salt e.g. $Co(NO_3)_2$ as catalyst (entries 9 & 10).

Further studies showed that the amount of PPh_3 added for pyrolysis to obtain the catalyst Co@NPC had a profound influence on the reduction efficiency (Figure 2). Upon addition of 1 wt% of PPh_3, the conversion of nitrobenzene was boosted substantially from 41 to 60%, further increase of the added amounts led to gradual improvement in activity without significant influence on selectivity to desired aniline. However, an optimal amount to be 20 wt% existed and a decrease in catalytic performance was observed with further more increase of the amount of PPh_3. For clarity, all catalysts for characterization and catalytic test are based on 20 wt% of PPh_3 thereinafter unless otherwise noted.

Given such impressive findings, great efforts were devoted to gain profound insight into the structure of the catalyst Co@NPC and to correlate the relationship between structure and catalytic performance. X-ray diffraction (XRD) characterization disclosed that the metallic cobalt was predominantly generated after pyrolysis with characteristic diffraction peak appearance at 44.2, 51.5, and 75.9°, assignable to the (111), (200), and (220) facets of structured metallic cubic cobalt (JCPDS No. 15-0806). Besides, a characteristic bump diffraction peak at around 25° corresponding to the (002) plane of graphitic carbon was also observed (Figure 3a). The almost same XRD pattern was observed for the catalyst Co@NC-800. These observations are critically different from the previously reported examples,[7] in which the mixed cobalt phases including metallic Co, CoO, and Co_3O_4 were formed simultaneously. Such discrepancy clearly indicates that this pyrolysis reduction strategy directly derived from biomass as C and N sources could manufacture metallic cobalt with nice crystallinity. Notably, for the catalysts with N-doping or N,P-codoping, in particular for the cases of Co@NPC-x with variable pyrolysis temperature, tiny diffraction peak at 40.6° appeared (Figure S1, Supporting Information). Similarly, the tiny peak at 40.6° was also detected for the catalysts Co@NPC-800 with different PPh_3 added amounts, especially for the catalysts with larger than 5 wt% amounts (Figure S2, Supporting Information). However, such peak is not observed for the sample Co@C-800, suggesting the interaction between cobalt NPs and heteroatoms in the carbon matrix to most likely form Co-P, or Co-N_x, or their mixture phases.[11]

Field emission scanning electron microscopy (FE-SEM) and transmission electron microscopy (TEM) observation of the Co@NPC-800 demonstrated that the formation of uniform spherical particles with a diameter of around ca. 23 nm (Figure 3b-f). Further high-resolution (HR) TEM analysis revealed a highly integrated nanostructure of the layered graphitic carbon-coated cobalt NPs (Figure 3f). The well-resolved lattice spacing of 0.205 and 0.338 nm corresponding to the (111) and (002) plane of the metallic cobalt and graphitic carbon can be perceived, respectively, which is in good line with the XRD observation. A high-angle annular dark-field scanning transmission electron microscopy (HAADF-STEM) images with sub-Ångström resolution further confirmed that uniform cobalt NPs were formed (Figure 3g), and the corresponding energy-dispersive X-ray (EDX) maps showed that Co, N, P, and C atoms were distributed homogeneously within the catalyst (Figure 3h-k). Magnetic measurements also confirmed the formation of metallic cobalt NPs (Ms = 6.2 emu/g, T = 300 K), which is particularly helpful for simple separation with external magnet after reaction (Figure S10).

View Article Online
DOI: 10.1039/C8GC00619A

The formation of graphitic carbon was further proved by the Raman spectrum (Figure 4a), in which the G band at 1590 cm^{-1} indicates the in-plane vibration of the sp^2 carbon atoms, while the D band at 1350 cm^{-1} is a defect-induced nonperfect crystalline structure of the material.[12] The I_G/I_D (I_D and I_G signify the intensity of D and G band) ratio of the Co@NC-800 to be 1.03 is slightly higher than that of Co@NPC-800 (1.01), indicative of more structural defects and disordered graphitic carbon due to N and P atoms dually incorporated into the resulting carbon lattices.[13] Such trend agreed well with the observation for the Co@NPC-800 with varying P contents (Figure S5). Similarly, increasing the pyrolysis temperature (700, 800, and 900°C) for the Co@NPC-x led to relatively higher degree of graphitization (Figure S4). N_2 adsorption/desorption measurements clearly demonstrated that the catalysts prepared in this strategy possess hierarchically micro-, meso-, and macro-pores with high specific surface areas and large pore volumes as shown in Figure 4b, Figure S3, and Table S7 in the Supporting Information, which are expected to favor the rapid mass-transfer and can provide sufficient active sites exposure for catalysis. Remarkably, the catalyst Co@NPC-800 showed a relatively higher surface area than Co@NC-800, indicating that the second P-doping is significantly beneficial to the pores formation during pyrolysis,[14] thereby leading to a great increase in surface area.

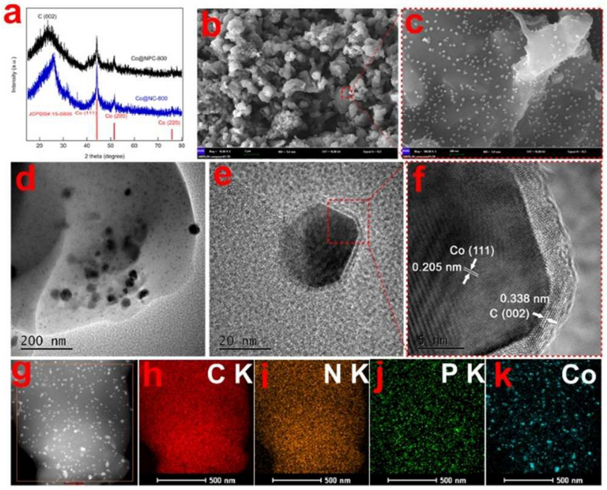

Figure 3. a) X-ray diffraction patterns for the catalysts Co@NC-800 and Co@NPC-800; b, c) SEM images of Co@NPC-800. The magnified image in (c) clearly reveals the uniformly sized nanospheres. d, e, f) HR-TEM image of Co@NPC-800 with different maganitute, showing the carbon shells and coated metal nanoparticles. Inset (f): cystal (111) plane of the metallic Co and (002) plane of the carbon. g-k) HAADF-STEM image and corresponding EDX maps of Co@NPC-800 for C (h), N (i), P (j), and Co (k).

X-ray photoelectron spectroscopy (XPS) was carried out to further investigate the surface compositions and chemical state of the Co@NPC (Figure 4c-e). The XPS survey spectrum clearly showed the obvious signals of N, P, C, O, and Co elements without other impurities. Four types of N, including graphitic (401.5 eV, 21.4%), pyrrolic (400.2 eV, 31.5%), Co-N$_x$ (399.7 eV, 12.6%), and pyridinic (397.8 eV, 34.5%), could be distinguished from N 1s spectrum (Figure 4c).[15] Pyrrolic-N and pyridinic-N species in Co@NPC-800 catalyst are the dominant peaks in the N 1s XPS spectrum, which not only are favorable for the reduction, but also serve as anchoring sites for formation of Co-N$_x$ sites. Notably, the Co-N$_x$ species in all samples was observed, indicating the coordination interaction between Co NPs and N in the carbon framework, which is believed to improve the catalytic activity. The XPS 2p spectrum (Figure 4d) in Co@NPC-800 shows deconvoluted peaks at 129.3, 130.2, 132.4, corresponding to the P 2p$_{3/2}$, P 2p$_{1/2}$, P-C bond, and a peak at 133.4 eV could be assigned to the P-O oxidized species of phosphide due to the inevitable oxidation in the storage.[16] The Co 2p XPS spectrum was fitted into four peaks at 778.5, 780.3, 782.7, and 785.4 eV (Figure 4e). The peaks at 778.5 and 129.3 eV are close to the binding energies of Co and P in CoP,[17] and the BE of Co 2p$_{3/2}$ has positive shift and P 2p$_{3/2}$ has negative shift, respectively, compared with the BE of metallic Co (778.1 eV) and elemental phosphorus (130.0 eV). Such results suggest that Co and P in catalyst Co@NPC-800 have a partial positive charge (δ^+) and negative charge (δ^-), respectively, which results from the electron transfer from Co to P.[18] In contrast, only metallic Co and oxidized Co peaks were observed in Co 2p XPS spectrum for the catalyst Co@NC-800 (Figure S9). In addition, the BE of 132.4 eV for P-C further demonstrates the doping of additional P into N-doped carbon lattices. Note that the content percentage of P 2p peaks assignable to CoP and P-C species gradually increased when the amount of PPh$_3$ was enhanced or the pyrolysis temperature increased (Figure S6-8), suggesting more P atoms incorporate into the carbon lattices, thereby increasing the contents of Co-P species in the catalysts.

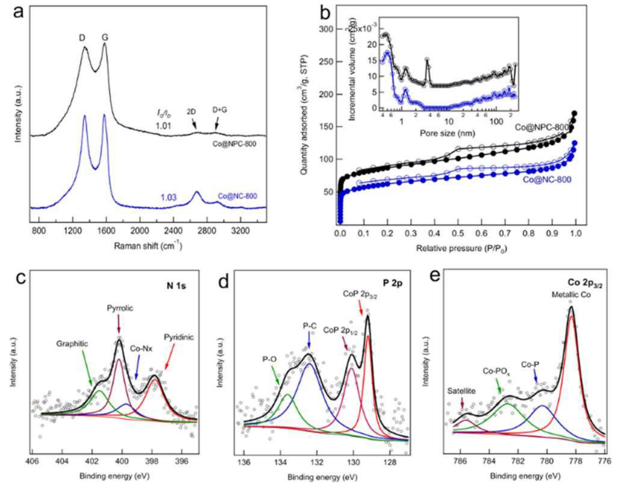

Figure 4. a) Raman spectroscopy for the catalysts Co@NC-800 and Co@NPC-800; b) N2 sorption isotherms of the catalysts Co@NC-800 and Co@NPC-800 at 77 K, and the inset is corresponding pore size distributions calculated using a nonlocal density function theory (NLDFT) method; d) Magnetic hysteresis loops of Co@NPC-800 at 300 K, and the inset is the illustration of magnetic separation of the catalyst from solution with external magnet; c) N 1s, d) P 2p, and e) Co 2p spectra of Co@NPC-800 catalyst.

Taken all characterization results together, such a geometric confinement of Co NPs within N,P-codoped graphitic carbon shells is believed that: 1) N and P heteroatoms in the carbon framework can serve as active sties beneficial for interacting with functionalized nitroarenes substrate and activating FA or ammonium formate, which was truly reflected by the difference in catalytic performance among the supports of activate carbon, NC-800, and NPC-800 as catalyst, respectively (Table 1, entries 6-8); 2) a synergistic effect between Co NPs and N,P-dopants in the carbon

View Article Online
DOI: 10.1039/C8GC00619A

framework to form Co-P, Co-N_x, or their mixture species, integrally allows it to significantly boost the reaction efficiency in combination with the N,P-dopants as active sites.

Table 2. Substrate scope of functionalized nitroarenes.[a]

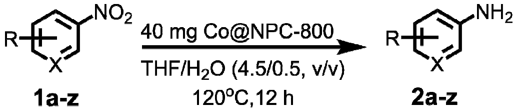

Entry	Substrate		Conversion (%)	Selectivity (%)	Entry	Substrate		Conversion (%)	Selectivity (%)
1	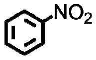	(**1a**)	100	97	14	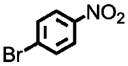	(**1n**)	100	>99
2	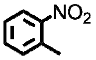	(**1b**)	100	>99	15	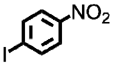	(**1o**)	100	>99
3	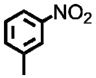	(**1c**)	100	>99	16	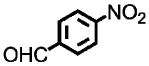	(**1p**)	100	>99
4		(**1d**)	100	>99	17	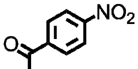	(**1q**)	100	>99
5	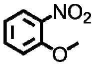	(**1e**)	95	>99	18	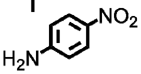	(**1r**)	100	>99
6	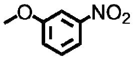	(**1f**)	100	>99	19	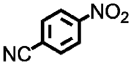	(**1s**)	100	>99
7	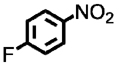	(**1g**)	100	>99	20	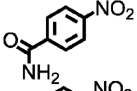	(**1t**)	100	>99
8	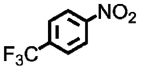	(**1h**)	100	>99	21	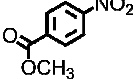	(**1u**)	100	>99
9	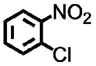	(**1i**)	100	>99	22	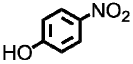	(**1v**)	100	>99
10	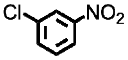	(**1j**)	100	>99	23	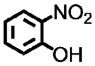	(**1w**)	100	>99
11	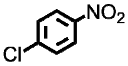	(**1k**)	100	>99	24	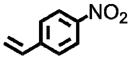	(**1x**	100	>99
12	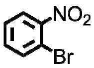	(**1l**)	100	>99	25	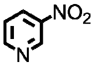	(**1y**)	100	>99
13	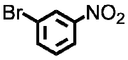	(**1m**)	100	>99	26	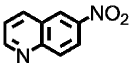	(**1z**)	99	>99

Reaction conditions: nitro compound (0.5 mmol), $HCOONH_4$ (2.0 mmol), Co@NPC-800 (40 mg, 4.8 mol% of Co), THF/H_2O (4.5/0.5, v/v, mL), 120°C, 12 h. Conversion and selectivity were determined by GC-FID using dodecane as an internal standard. The product was structually confirmed by using an authentic sample.

Subsequently, we investigated the substrate scope to explore the general applicability of this catalytic transfer hydrogenation protocol under the optimized conditions (Table 2). In general, the catalyst Co@NPC-800 enabled the reduction of a diverse array of functionalized nitroarenes, consistently providing the corresponding anilines in high yields with exclusive selectivity. Electron-donating and electron-withdrawing substituents at the *o*-, *m*-, *p*-positions on the phenyl ring of nitroarenes all gave high yields to their corresponding anilines, suggesting that the electronic and/or steric effect of substituents on aromatic rings is negligible. More importantly, for halogenated nitrobenzenes, full conversion is achieved, giving excellent yields of the target product. The position of the halide substituent did not induce any significant differences in reactivity, and no dehalogenation processes are observed for all halogenated substrates. Gratifyingly, nitroarenes bearing amine, hydroxyl, cyano, or ester, amide substituents were all tolerated by this protocol, giving the corresponding anilines in >99% yield without any signs of side products. Particularly, the nitroarenes decorated with the most challenging reducible functional groups, such as aldehyde, ketone, nitrile, and C=C, were successfully reduced to the aniline

View Article Online
DOI: 10.1039/C8GC00619A

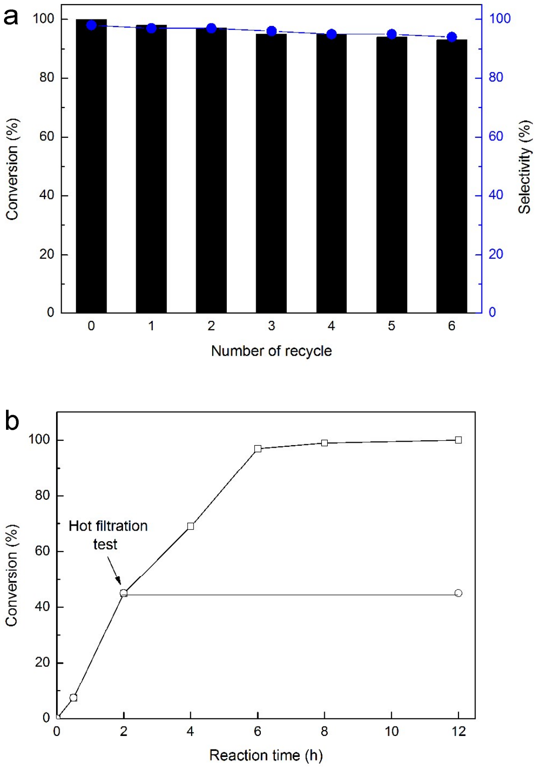

Figure 5. a) Recycling and b) hot filtration test of the catalyst Co@NPC-800 for catalytic transfer hydrogenation of nitrobenzene to aniline.

Reaction conditions: nitrobenzene (0.5 mmol), $HCOONH_4$ (2 mmol), Co@NPC-800 (40 mg, 4.8 mol% of Co), THF/H_2O (5 mL, 4.5/0.5, v/v), 120°C, 12 h.

products with exclusive selectivity and maintained the reducible groups untouched, highlighting the excellent chemoselectivity of the nanostructured core-shell cobalt NPs catalyst and the remarkable advantage compared to that of noble metal-based catalysts. In addition, heteroatom-containing nitroarenes can also be efficiently reduced to their corresponding anilines, which are in particular important intermediates in the pharmaceutical and agrochemical industries.

Durability/recyclability of a catalyst is critical for practical applications. Upon completion of the reduction of nitrobenzene, the catalyst Co@NPC-800was recollected using simple external magnet, washed, and dried for subsequent cycles. As shown in Figure 5a, the activity and selectivity remained with negligible changes after five recycling experiments, demonstrating the high durability of this catalyst. The heterogeneity of Co@NPC-800 was further confirmed by hot filtration test (Figure 5b). We carried out the reduction of nitrobenzene and removed the catalyst from the reaction mixture by hot filtration at approximately 45% conversion of nitrobenzene. After removal of the Co@NPC-800 catalyst, the filtrate was again held at 120°C for continuing reaction. In this case, no additional conversion increment of nitrobenzene was observed, indicating that leached Co NPs or other Co-species from the catalyst (if any) are not responsible for the observed activity. It was confirmed by ICP-OES analyses that the amounts of Co that leached into the supernatant after the first run were not detectable (below the detection limit). These tests rule out the role of any leached Co nanoparticles or other Co-species in catalyzing catalytic transfer hydrogenation reaction.

To shed insight into the possible pathway of the catalytic transfer hydrogenation of nitroarenes, additional experiments were carried out (Scheme S1, Supporting Information). The reduction of nitrobenzene in the presence of an atmosphere of molecular hydrogen instead of formic acid or ammonium formate as hydrogen donor didn't proceed under otherwise identical conditions, indicating that nitrobenzene is reduced by in-situ generated cobalt hydride species rather than molecular hydrogen. No hydrogen was detected out for the headspace gas after reaction by GC-TCD analysis, in further support of the cobalt hydride formation. It was widely accepted that the nitrogen atoms in the metal modified N-doped carbon catalysts act as base sites.[7b,19] To confirm this assumption, the reaction was carried out with identical equivalent of $HCOONH_4$ and H_3PO_4. In this case, 51% conversion of nitrobenzene with exclusive selectivity to **2a** was observed; while 97% conversion with 98% selectivity to **2a** was achieved without addition of H_3PO_4 under otherwise identical conditions. This result clearly indicates that H_3PO_4 as a stronger acidity more readily neutralizes the nitrogen atoms to form NH^+, thus partially deactivating the Co@NPC-800 catalyst. Accordingly, the catalyst Co@NC-800 was treated with the same manner for the benchmark reaction and only gave 7% conversion of **1a**, which is comparable to the catalytic performance of the catalyst Co@C-800 without N doping under identical conditions. We further prepared the catalysts Co@NC-800 by pyrolysis of the mixture of activated carbon and $CoCl_2$ with exogenous addition of melamine as N source at 800°C under N_2 atmosphere. Their respective catalytic performance for benchmark reaction shows a high dependence on N content and superior catalytic efficiency is obviously achieved with higher N content. These results firmly indicate that N atoms indeed played an essential role in catalysis.

Meanwhile, to distinguish the role of P dopant in the catalyst, we prepared the catalyst Co@PC-800 by direct pyrolysis of the mixture of activated carbon, $CoCl_2$ and PPh_3 (20 wt%, an optimal P content in the catalyst Co@NPC-800) as P source with the same preparation procedure. The resultant catalyst showed 79% of conversion of **1a** with 100% selectivity to **2a** under standard conditions, which is inferior to that of Co@NPC-800 while considerably higher than that of Co@C-800. This result further confirms the boosting role of P atoms for the reaction efficiency. Furthermore, head-to-head comparison demonstrates that the catalysts Co@C-800, Co@NC-800, and Co@NPC-800 are significantly higher in activity than their corresponding supports AC-800, NC-800 and NPC-800, clearly verifying the critical role of Co NPs. Taken all these results into consideration, we strongly believe that it is the synergistic effect of multi-components among N, P, and Co NPs rather than either the heteroatoms or Co nanoparticles solely facilitate the reaction.

Given all control experiments, we tentatively proposed the plausible reaction mechanism as shown Scheme 1. In the first step, N atoms on the catalyst, as basic sites with remarkable role in facilitating proton transfer, can capture H^+ from the formic acid to generate NH^+ and form the Co-formate intermedidate. The formate anions tend to adsorb on the surface of Co NPs, as the formate anions could be coordinate with the empty d orbitals of Co owing to the low d-electron density of Co. In the second step, the Co-formate intermediate can produce a CO_2 molecule and in-situ form CoH^-. Due to the P doping, as a more electronegative atom and stronger

View Article Online
DOI: 10.1039/C8GC00619A

coordinating capacity, P can strongly coordinate with Co NPs, even to form CoP species, which has been elucidated by XPS characterizations. Such interaction resulted in the Co has a partial positive charge (δ^+) due to the electron transfer from Co to P, which is beneficial for the preferential adsorption of the oxygen atom in the NO_2 group and formate anions.[19b] In the third step, when nitroarenes is added in the catalytic system, two parts of the hydrogen in NH^+ and CoH^- prefer to react with the nitro groups to generate an aniline with no hydrogen detected, thereby completing the entire catalytic cycle.

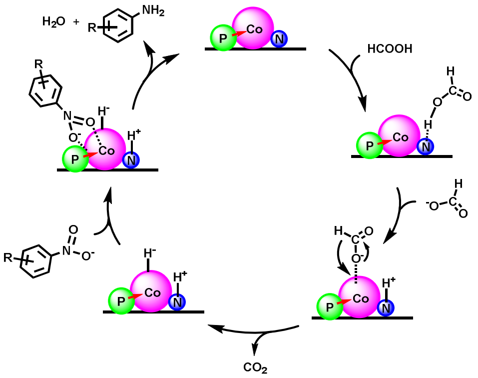

Scheme 1. Proposed mechanism for transfer hydrogenation of nitroarenes.

Conclusions

In conclusion, we developed a heterogeneous, inexpensive, and active cobalt NPs encapsulated with a N,P-codoped carbon shell derived from the biomass. The as-prepared catalysts possess large surface area, high pore volume with hierarchical micro-, meso-, and macro-pores structure. The synergism of N and P dopants on the graphitic carbon and confined Co NPs produces extremely high active sites for catalytic transfer hydrogenation of functionalized nitroarenes using formic acid or ammonium formate as hydrogen donor. The most active catalyst showed outstanding activity and a broad variety of functionalized nitroarenes can be efficiently reduced to their corresponding anilines with exclusive selectivity and great tolerance of functional groups. The catalyst also demonstrates high stability and can be easily separated using simple external magnet for at least 6 successive reuses without significant loss in both activity and selectivity. Hence, this study provides a new strategy for preparing biomass-derived multicomponent hybrid materials, which can be further applied in other organic transformations and are currently underway in our lab.

Conflicts of interest

There are no conflicts to declare.

Acknowledgements

We gratefully acknowledge the start-up financial support from Qingdao Institute of Bioenergy and Bioprocess Technology (QIBEBT), Chinese Academy of Sciences (Grant NO. Y6710619KL) and 13th-Five Key Project of the Chinese Academy of Sciences (Grant No. Y7720519KL). We thank Professor Xiufang Chen (QIBEBT) for generous supply of bamboo shoots.

Notes and references

1 a) Lawrence, S. A. Amines: Synthesis, Properties and Applications (Cambridge Univ. Press, 2004); b) Downing, R. S.; Kunkeler, P. J.; van Bekkum, H. *Catal. Today*, 1997, **37**, 121-136; c) Ono, N. The Nitro Group in Organic Synthesis (Wiley-VCH, 2001).

2 a) Corma, A.; Serna, P. *Science* 2006, **313**, 332-334; b) Blaser, H. U.; Steiner, H.; Studer, M. *ChemCatChem* 2009, **1**, 210-22; b) Jagadeesh, R. V.; Surkus, A.-E.; Junge, H.; Pohl, M.-M.; Radnik, J.; Rabeah, J.; Huan, H. M.; Schunemann, V.; Brückner, A.; Beller, M. *Science* 2013, **342**, 1073-1076; c) Zhang, S.; Chang, C.-R.; Huang, Z.-Q.; Li, J.; Wu, Z.; Ma, Y.; Zhang, Z.; Wang, Y.; Qu, Y. *J. Am. Chem. Soc.* 2016, **138**, 2629-2637; d) Wei, H. S.; Liu, X. Y.; Wang, A. Q.; Zhang, L. L.; Qiao, B. T.; Yang, X. F.; Huang, Y.Q.; Miao, S.; Liu, J. Y.; Zhang, T. *Nat. Commun.* 2014, **5**, 5643-5651; e) Nie, R. F.; Wang, J. H.; Wang, L. N.; Qin, Y.; Chen, P.; Hou, Z. Y. *Carbon* 2012, **50**, 586-596.

3 a) Siegrist, U.; Baumeister, P.; Blaser, H.-U. Chem. Ind. (Dekker) 1998, **75**, 207-210; b) Corma, A.; Serna, P.; Concepción, P. Calvino, J. J. *J. Am. Chem. Soc.* 2008, **130**, 8748-8753.

4 a) Zhou, P.; Zhang, Z. H. *ChemSusChem* 2017, **10**, 1892-1897; b) Liu, Z.; Dong, W. H.; Cheng, S. S.; Guo, S.; Shang, N. Z.; Gao, S. T.; Feng, C.; Wang, C.; Wang, Z. *Catal. Commun.* 2017, **95**, 50-53; c) Mei, N.; Liu, B. *Int. J. Hydrogen Energy* 2016, **41**, 17960-17966; d) Ma, X.; Zhou, Y-X.; Liu, H.; Li, Y.; Jiang, H.-L. A *Chem. Commun.* 2016, **52**, 7719-7722; e) Gawande, M. B.; Guo, H. Z.; Rathi, A. K.; Branco, P. S. Y.; Chen, Z.; Varma, R. S.; Peng, D.-L. *RSC Adv.* 2013, **3**, 1050-1054; f) Li, Y.; Zhou, Y.-X.; Ma, X.; Jiang, H.-L. *Chem. Commun.* 2016, **52**, 4199-4202.

5 Selected recent reviews: a) Morris, R. H. *Acc. Chem. Res.* 2015, **48**, 1494-1502; b) Chirik, P. J. *Acc. Chem. Res.* 2015, **48**, 1687-1695; c) Chakraborty, S.; Bhattacharya, P.; Dai, H.; Guan, H. *Acc. Chem. Res.* 2015, **48**, 1995-2003; d) He, L.; Weniger, F.; Neumann, H.; Beller, M. *Angew. Chem. Int. Ed.* 2016, **55**, 12582-12594 and references therein.

6 Westerhaus, F. A.; Jagadeesh, R. V.; Wienhöfer, G.; Pohl, M.-M.; Radnik, J.; Surkus, A.-E.; Rabeah, J.; Junge, K.; Junge, H.; Nielsen, M.; Brückner, A.; Beller, M. *Nat. Chem.* 2013, **5**, 537-543.

7 a) Wei, Z. Z.; Wang, J. S.; Mao, J.; Su, D. F.; Jin, H. Y.; Wang, Y. H.; Xu, F.; Li, H. R.; Wang, Y. *ACS Catal.* 2015, **5**, 4783-4789; b) Wang, X.; Li, Y. W. *J. Mol. Catal. A: Chem.* 2016, **420**, 56-65; c) Schwob, T.; Kempe, R. *Angew. Chem. Int. Ed.* 2016, **55**, 15175-15179; d) Zhang, F. W.; Zhao, C.; Chen, S.; Li, H.; Yang, H.Q.; Zhang, X.-M. *J. Catal.* 2017, **348**, 212-222; e) Liu, L. C.; Concepcion, P.; Corma, *J. Catal.* 2016, **340**, 1-9; f) Chen, F.; Surkus, A.-E.; He, L.; Pohl, M.-M.; Radnik, J.; Topf, C.; Junge, K.; Beller, M. *J. Am. Chem. Soc.* 2015, **137**, 11718-11724; g) Jagadeesh, R. V.; Murugesan, K.; Alshammari, A. S.; Neumann, H.; Pohl, M.-M.; Radnik, J.; Beller, M. *Science* 2017, **358**, 326-332.

8 a) Liu, W. G.; Zhang, L. L.; Yang, W. S.; Liu, X. Y.; Yang, X. F.; Miao, S.; Wang, W. T.; Wang, A. Q.; Zhang, T. *Chem. Sci.* 2016, **7**, 5758-5764; b) Zhou, P.; Zhang, Z. H.; Jiang, L.; Yu, C. L.; Lv, K. L. *Appl. Catal. B: Environ.* 2017, **210**, 522-532.

9 (9) a) Sahoo, B.; Surkus, A.-E.; Pohl, M.-M.; Radnik, J.; Schneider, M.; Bachmann, S.; Scalone, M.; Junge, K.; Beller, M. *Angew. Chem. Int. Ed.* 2017, **56**, 11242-11247; b) Bi, Q.-Y.;

View Article Online
DOI: 10.1039/C8GC00619A

Lin, J.-D.; Liu, Y.-M.; He, H.-Y.; Huang, F.-Q.; Cao, Y. *Angew. Chem. Int. Ed.* 2016, **55**, 11849-11853.

10 a) Ji, G.-J.; Duan, Y.-N.; Zhang, S.-C.; Fei, B.-H.; Chen, X.-F.; Yang, Y. *ChemSusChem* 2017, **10**, 3427-3434; b) Duan, Y.-N.; Ji, G.-J.; Zhang, S.-C.; Yang, Y. *Catal. Sci. Technol.* 2018, **8**, 1039-1050.

11 a) Das, D.; Nanda, K. K. *Nano Energy* 2016, **30**, 303-311. b) S. H. Ahn, A. Manthiram, *Small* 2017, 1702068-1702079.

12 Mhamane, D.; Ramadan, W.; Fawzy, M.; Rana, A.; Dubey, M.; Rode, C.; Lefez, B.; Hannoyerd, B.; Ogale, S. *Green Chem.* 2011, **12**, 1990-1996.

13 Qian, W.; Sun, F.; Xu, Y.; Qiu, L.; Liu, C.; Wang, S.; Yan, F. *Energy Environ. Sci.* 2014, **7**, 379-386.

14 Zhang, L.; Chen, X.-F.; Guan, J.; Jiang, Y.-J.; Hou, T.-G.; Mu, X.-D. *Mater. Res. Bull.* 2013, **48**, 3485-3491.

15 Hou, Y.; Qiu, M.; Zhang, T.; Ma, J.; Liu, S. H.; Zhuang, X. D.; Yuan, C.; Feng, X. L. *Adv. Mater.* 2017, **29**, 1604480-1604487.

16 Zhang, J. T.; Zhao, Z. H.; Xia, Z. H.; Dai, L. M. *Nat. Nanotechnol.* 2015, **10**, 444-452.

17 Jiang, P.; Liu, Q.; Liang, Y. H.; Tian, J.Q.; Xing, Z. C.; Asiri, A. M.; Sun, X. P. *Angew. Chem. Int. Ed.* 2014, **53**, 12855-12859.

18 Wu, G.; More, K. L.; Johnston, C. M.; Zelenay, P. *Science* 2011, **332**, 443-446.

19 a) Zhou, P.; Zhang, Z. H.; Jiang, L.; Yu, C. L.; Lv, K. L.; Sun, J.; Wang, S. G. *Appl. Catal. B: Environ*, 2017, **210**, 522-532. b) Liu, X. M.; Cheng, S. J.; Long, J. L.; Zhang, W.; Liu, X. H.; Wei, D. P. *Mater. Chem. Front.* 2017, **1**, 2005-2012.

View Article Online
DOI: 10.1039/C8GC00619A

Table of Contents

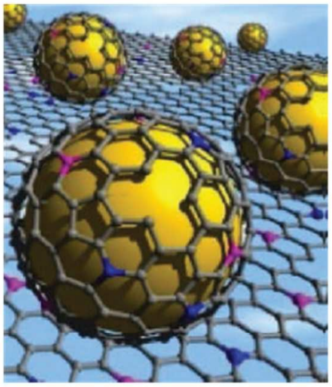

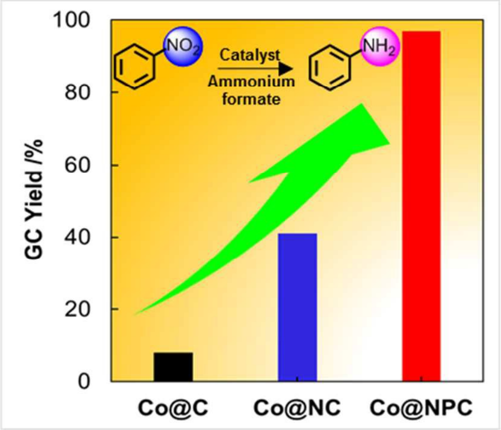

- A heterogeneous cobalt nanoparticles coated by N,P-codoped carbon shell
- 26 examples of functionalized nitroarenes
- Excellent activity and exclusive selectivity
- A broad functional groups tolerance
- Reusable and easy separation with external magnet